

# The Influence of Surface Roughness on the Electric Conduction Process in Amorphous Ta<sub>2</sub>O<sub>5</sub> Thin Films

Y. S. Kim,<sup>a</sup> M. Y. Sung,<sup>a</sup> Y. H. Lee,<sup>b</sup> B. K. Ju,<sup>b</sup> and M. H. Oh<sup>b</sup>

<sup>a</sup>Department of Electrical Engineering, Korea University, 1,5-Ka Anam-dong, Sungbuk-ku, Seoul 136-701, Korea

<sup>b</sup>Electronic Materials and Devices Research Center, Korea Institute of Science and Technology, Seoul, Korea

Amorphous Ta<sub>2</sub>O<sub>5</sub> thin films were deposited by radio-frequency magnetron sputtering at the substrate temperatures of 100, 200, and 300°C, respectively. The electrical properties of Ta<sub>2</sub>O<sub>5</sub> thin films were investigated as a function of substrate temperature and film thickness. The leakage current of the Ta<sub>2</sub>O<sub>5</sub> films was in the order of 10<sup>-5</sup> to 10<sup>-6</sup> A/cm<sup>2</sup> for an applied field of 1 MV/cm. The charge storage capacitances ( $\epsilon E_{\text{breakdown}}$ ) were 7.7 (100°C), 7.9 (200°C), and 3.7 (300°C)  $\mu\text{C}/\text{cm}^2$ . Most of the electrical analyses were performed with the data obtained for the Ta<sub>2</sub>O<sub>5</sub> thin films deposited at 200°C substrate temperature because they showed optimum electrical properties. The dominant conduction mechanism changed from Schottky emission current at low field to Poole-Frenkel current at the high field. With increasing film thickness, the surface roughness increased, whereas the transition fields from the electrode-limited current to the bulk-limited current process decreased. To verify the effect of this surface roughness on the electrical conduction mechanism, a two-dimensional numerical simulator, MEDICI, was used to simulate the electric field distribution at the bulk region of the thin film and the interface region between the thin film and electrode.

© 1999 The Electrochemical Society. S0013-4651(98)11-090-X. All rights reserved.

Manuscript submitted November 30, 1998; revised manuscript received April 11, 1999.

Amorphous tantalum oxide (Ta<sub>2</sub>O<sub>5</sub>) thin films are being used widely in industry as dielectric layers for thin-film capacitors.<sup>1</sup> Ta<sub>2</sub>O<sub>5</sub> thin films have many outstanding characteristics, including a high capacitor density and high dielectric constant, and good refractive index match to ZnS for ac thin-film electroluminescent devices.<sup>2</sup> Their dielectric properties, especially their dc electrical conduction characteristics, have been studied a great deal and numerous reports have been published. However, their leakage current level still poses a serious limitation for practical applications.<sup>3-6</sup> In addition, relatively little knowledge about the electrical properties of sputtered Ta<sub>2</sub>O<sub>5</sub> in conjunction with structural parameters, such as surface roughness, implies that more detailed studies are needed in order to improve the properties of the films.

Many investigations have been carried out regarding the influence of the metal-insulator roughness on breakdown<sup>7-9</sup> but study has not been done with regard to its effect on current-voltage characteristics.

In this work, Ta<sub>2</sub>O<sub>5</sub> thin films were deposited by a radio-frequency (rf) magnetron sputtering technique. We studied the electrical properties, especially the mechanism of current conduction. An attempt was made to clarify the effect of actual Al-Ta<sub>2</sub>O<sub>5</sub> interface roughness on the current conduction process with reference to atomic force microscopy (AFM) analysis as well as two-dimensional numerical simulation. It was confirmed that the electric field distribution in the Ta<sub>2</sub>O<sub>5</sub> films, evaluated using the MEDICI simulator, agreed with the current-voltage characteristics of the Ta<sub>2</sub>O<sub>5</sub> thin films as a function of surface roughness.

## Experimental

The Ta<sub>2</sub>O<sub>5</sub> thin films were prepared by a rf-magnetron sputtering technique onto glass (Corning 7059) coated with a transparent electrode, indium-tin oxide (ITO), which has a sheet resistance of about 20  $\Omega/\square$ . A 4 in. Ta<sub>2</sub>O<sub>5</sub> ceramic disk sputtering target with 99.99% purity was used. The base pressure in the chamber was adjusted to  $2 \times 10^{-6}$  Torr, and the Ar (80%) and O<sub>2</sub> (20%) gas mixture pressure during the deposition was maintained at  $1 \times 10^{-2}$  Torr.

Three types of samples were prepared by varying the deposition temperature (100, 200, and 300°C) for the amorphous-Ta<sub>2</sub>O<sub>5</sub> thin films. The effect on the electric properties of Ta<sub>2</sub>O<sub>5</sub> was investigated as a function of the thickness (200, 300, and 400 nm) for the thin films deposited at 200°C substrate temperature. An aluminum electrode of 0.7 mm diam was formed on the thin films by thermal evaporation and then the electric properties of the capacitors with metal-insulator-metal structure (Al/Ta<sub>2</sub>O<sub>5</sub>/ITO) were investigated.

The surface morphologies of the Ta<sub>2</sub>O<sub>5</sub> thin films were studied using AFM analysis. The dielectric properties, such as capacitance

and dielectric loss, were measured by an impedance analyzer (HP 4912A). The current-voltage characteristics were obtained by a Keithley 237 high-voltage source and measurement unit.

## Results and Discussion

*Characteristics of Ta<sub>2</sub>O<sub>5</sub> as a function of substrate temperature.*—Figure 1 shows the dielectric constant and loss factor of amorphous Ta<sub>2</sub>O<sub>5</sub> thin films as a function of the substrate temperature during deposition. The dielectric constants are from 22 to 26 and are nearly independent of frequency in the range 1-100 kHz. The loss factors increase with increasing the substrate temperature at high frequency.

Optical transmittance was also investigated for the Ta<sub>2</sub>O<sub>5</sub> thin films on the ITO-coated glass for different substrate temperatures during deposition, as shown in Fig. 2. The transmittance of the thin films in the visible range was in the range 80-90%, regardless of substrate temperature. From these data, the calculated indexes of refraction were 1.9-2.4.

Leakage current is a critical issue in semiconductor device application. Figure 3 shows the current-voltage (I-V) characteristics of the Ta<sub>2</sub>O<sub>5</sub> thin film as a function of deposition temperature. The voltage was applied with a step of 0.5 V. The leakage currents of Ta<sub>2</sub>O<sub>5</sub> are of the order of 10<sup>-5</sup>-10<sup>-6</sup> A/cm<sup>2</sup> at 1 MV/cm applied field. The

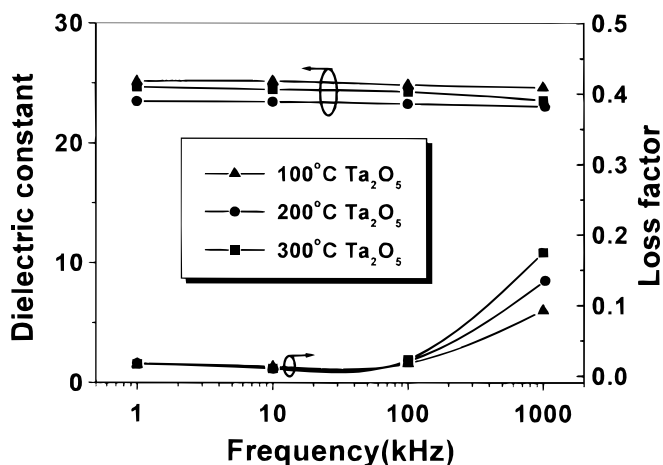


Figure 1. Frequency dependence of the dielectric constant for Ta<sub>2</sub>O<sub>5</sub> thin films.

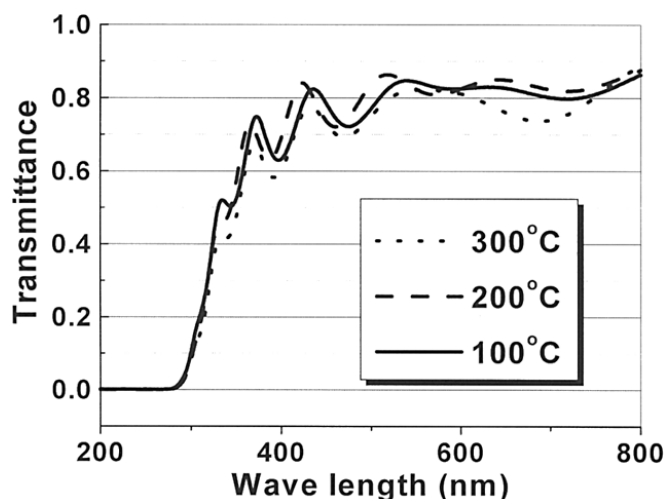


Figure 2. Optical transmittance of the Ta<sub>2</sub>O<sub>5</sub> thin films.

insulating layer for semiconductor devices and other applications should have low leakage current as well as high charge-storage capacitance ( $\epsilon E_{\text{breakdown}}$ ) in order to achieve both low power consumption and stable operation of the device. The charge-storage capacitances are 7.7 (100°C), 7.9 (200°C), and 3.7 (300°C)  $\mu\text{C}/\text{cm}^2$ . The electrical characteristics of all Ta<sub>2</sub>O<sub>5</sub> thin films, except the thin film with 300°C deposition temperature, show very good characteristics for the semiconductor devices, especially the ac thin-film electroluminescent device (ACTFELD). Regarding the leakage current and the charge-storage capacitance, it is reasonable to select the optimum substrate temperature as 200°C.

*I-V characteristics of Ta<sub>2</sub>O<sub>5</sub> thin films.*—The leakage current in a dielectric film can be due to several conduction mechanisms. DC electrical conduction in the dielectric films can be described in terms of the electrode-limited or bulk-limited processes.

Voltage polarity dependence of the leakage current is observed for the Ta<sub>2</sub>O<sub>5</sub> thin films with 200°C deposition temperature in Fig. 4. The leakage current is independent of the voltage polarity for high electric field (region 1), as shown in Fig. 4. The current invariance with the voltage polarity could be explained by a bulk-limited current process, but the leakage current is dependent on voltage polarity at low electric field (region 2). For the electrode-limited current, the current is dependent on voltage polarity. This is attributed to the difference in work function of the top and bottom electrodes.

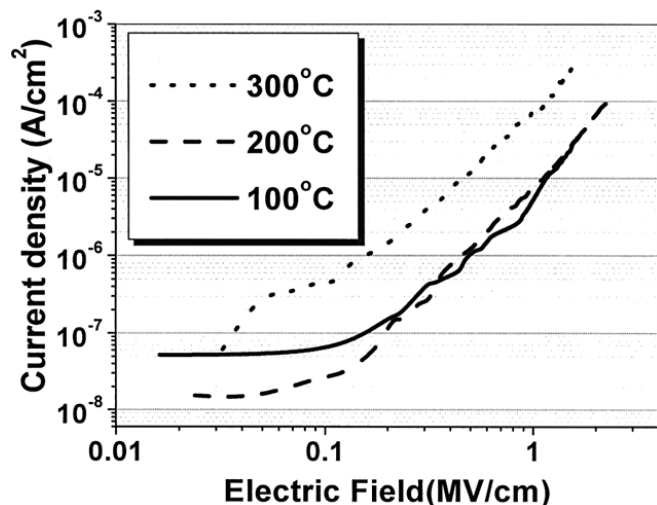


Figure 3. I-V characteristics of amorphous Ta<sub>2</sub>O<sub>5</sub> thin films as a function of substrate temperature during deposition.

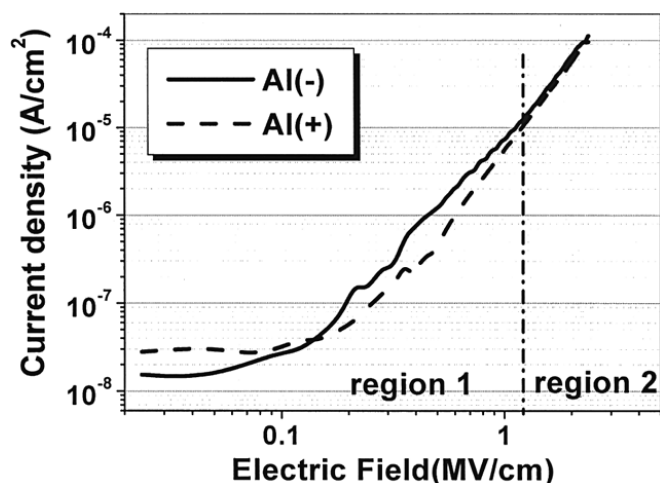


Figure 4. Polarity dependence of the leakage current for Ta<sub>2</sub>O<sub>5</sub> thin films with 200°C substrate temperature during deposition.

In addition, film thickness dependence of the leakage current must be considered. Ta<sub>2</sub>O<sub>5</sub> films with different thicknesses were prepared by varying the deposition time. The thicknesses of the Ta<sub>2</sub>O<sub>5</sub> thin films were 200 nm (sample 1), 300 nm (sample 2), and 400 nm (sample 3). To determine the dominant mechanism of the leakage current, the current-voltage characteristics of the Ta<sub>2</sub>O<sub>5</sub> thin films were measured as a function of the film thickness. Figure 5 plots the logarithmic current density as a function of the square root of the electric field [ $\ln(J)$  vs.  $E^{1/2}$ ]. For low electric field (<2 MV/cm) a straight line can be obtained for samples 1 and 2, and there is very little thickness dependence of leakage current. This is further evidence for electrode-limited current, which is a Schottky emission (SE) process across the interface between the metal and an insulating film as a result of barrier lowering due to the applied field and image force. Thus, the dominant conduction mechanism at a low field for samples 1 and 2 is determined to be a Schottky emission process. At a high field (>2 MV/cm) the leakage current curve is slightly deviated from straight line for samples 1 and 2.

For sample 3, the thickness dependence of the leakage current is shown at over 0.3 MV/cm. To investigate these results, the insets of Fig. 5 and 6a plot the logarithmic current density divided by the electric field as a function of the square root of the electric field [ $\ln(J/E)$  vs.  $E^{1/2}$ ]. The subsequent curves are straight lines at a high electric field. The value of the dynamic dielectric constant that fits the opti-

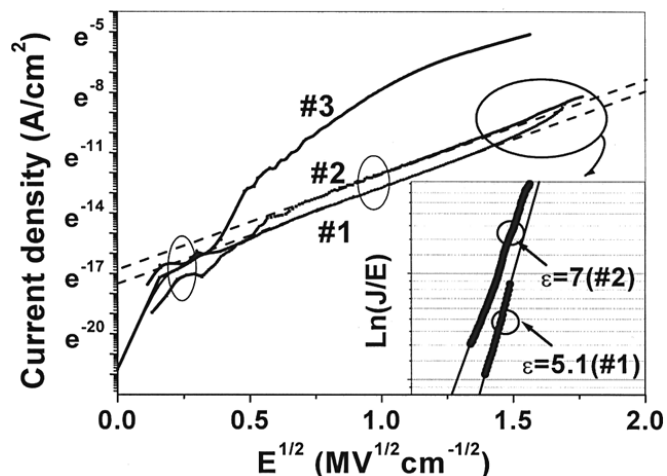
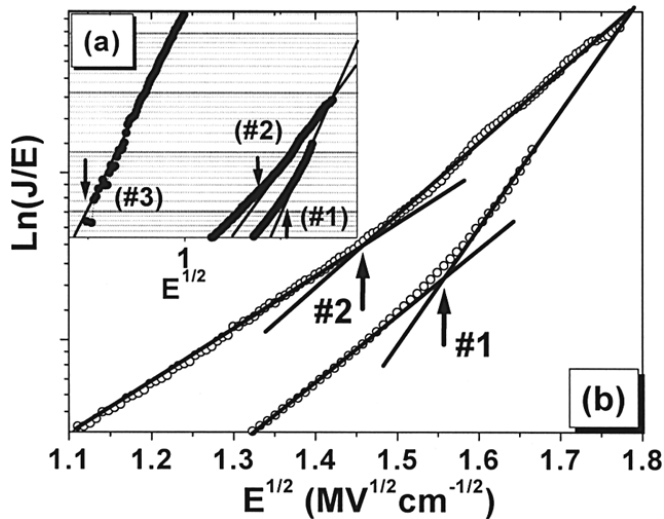


Figure 5.  $\ln(J)$  vs.  $E^{1/2}$  plot for the amorphous Ta<sub>2</sub>O<sub>5</sub> thin films. The inset figure is  $\ln(J/E)$  vs.  $E^{1/2}$  plot for the amorphous Ta<sub>2</sub>O<sub>5</sub> thin films in the high field region for samples 1 and 2.



**Figure 6.** (a)  $\ln(J/E)$  vs.  $E^{1/2}$  plot for the amorphous  $\text{Ta}_2\text{O}_5$  thin films in the high field region and transition field for samples 1, 2, and 3. (b) The definition of transition field for samples 1 and 2.

cal dielectric constant from the slope of the straight lines<sup>11-13</sup> was found to be 5.1 for sample 1, 7 for sample 2, and 4.4 for sample 3. These values agree with the optical dielectric constant obtained from the transmission spectrum. Hence, the dominant conduction mechanism at a high field is the Poole-Frenkel (PF) conduction mechanism. According to these results, the conduction process of amorphous  $\text{Ta}_2\text{O}_5$  thin films changes from being the electrode-limited current (SE current) at low field to being the bulk-limited current (PF current) at high field, which agrees with other reports.<sup>3,5,14</sup> These processes have three distinct voltage regions to consider: (i) low voltage where the characteristic is determined purely by the thermal processes (region a); (ii) intermediate voltage where the conduction process is electrode-limited and in which (a) contact tunneling and/or (b) impact ionization occur (region b); and (iii) high voltage where the characteristic is determined by the bulk region (region c).<sup>14</sup>

**Effect of surface roughness on I-V characteristics.**—In Fig. 6b we defined the transition field as an electric field of intersection of the slope of the bulk-limited current (PF current) and that of the electrode-limited current (SE current). The transition field for samples 1, 2, and 3 are seen in Fig. 6a. It is notable that the transition fields from the electrode-limited to the bulk-limited conduction process decreases with increasing film thickness. The transition fields for samples 1, 2, and 3 were 2.2, 1.9, and 0.27 MV/cm for the samples deposited to 200, 300, and 400 nm thickness, respectively.

Figure 7 shows the surface roughness of the  $\text{Ta}_2\text{O}_5$  thin films on the ITO with 0.98 nm surface roughness according to the different thicknesses by AFM analysis. The AFM results are summarized in Table I. The roughness increases with increasing thickness of the  $\text{Ta}_2\text{O}_5$  layer, because the peaks on the uneven growing surface receive more incident flux than the valley and the nucleus growth at the valley decreases in the rf-sputtered insulator. Figure 8b shows the root-mean-square (rms) roughness ( $\rho$ ) as a function of thickness ( $t$ ) of  $\text{Ta}_2\text{O}_5$  thin films. The dynamic scaling theory<sup>15</sup> predicts  $\rho \propto \langle t \rangle^\beta$  where  $\rho$ ,  $t$ , and  $\beta$  are rms roughness, film thickness, and the growth exponent of  $\text{Ta}_2\text{O}_5$  films, respectively. The  $\log(\rho)$  vs.  $\log(t)$  plot for each value of  $\langle t \rangle$  yielded a straight line with  $\beta = 0.3$ . The rms roughness of  $\text{Ta}_2\text{O}_5$  thin films scales with film thickness as a power law.

The transition field of the  $\text{Ta}_2\text{O}_5$  thin films was investigated as a function of surface roughness and thickness, as shown in Fig. 8a. It is noted that the transition fields are linearly dependent on the rms value of surface roughness evaluated by AFM, but there is no linearity of the relationship between the thickness and the transition field. It is reported that at region b (transition field region) one of two processes can occur. The field emission from the electrode into the

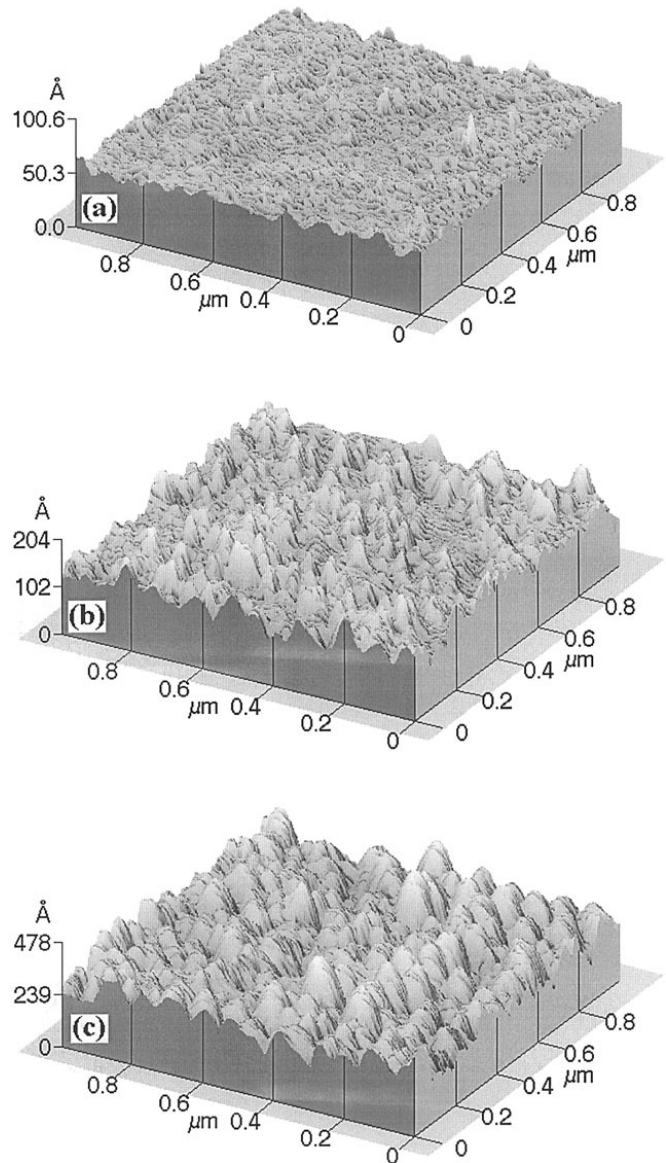


**Figure 7.** AFM image of  $\text{Ta}_2\text{O}_5$  thin films in  $1 \times 1 \mu\text{m}$  square regions: (a) 200, (b) 300, (c) 400 nm.

conduction band of the insulator can occur, or the impact ionization can occur in the contact region of the insulator.

In these results the contact resistance decreases rapidly with increasing voltage bias. This means that the process from region a to region b related to the surface properties. When this occurs, the applied field is shared equally between the contact and the bulk. Thereafter, all the voltage in excess of the transition field falls across the bulk, which is leading to a bulk-controlled process region c.<sup>14</sup>

To verify this surface effect on the electric field in the surface and the bulk of the  $\text{Ta}_2\text{O}_5$  thin film, a two-dimensional (2D) numerical simulator, MEDICI, was used to simulate the electric field distribu-

**Table I.** Roughness parameters of AFM images for  $\text{Ta}_2\text{O}_5$  thin films.

$\text{Ta}_2\text{O}_5$ Thickness	rms (nm)	Average (nm)
1 (200 nm)	1.1	0.85
2 (300 nm)	2.1	1.6
3 (400 nm)	10.4	3.02



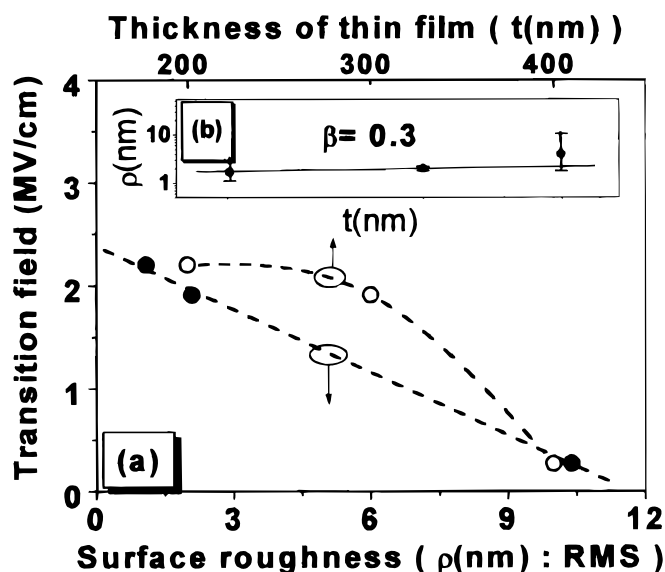


Figure 8. (a) Transition field from electrode-limited to bulk-limited current as functions of rms values obtained by AFM and thickness of Ta<sub>2</sub>O<sub>5</sub> thin films. (b) Plot of rms roughness as a function of thickness.

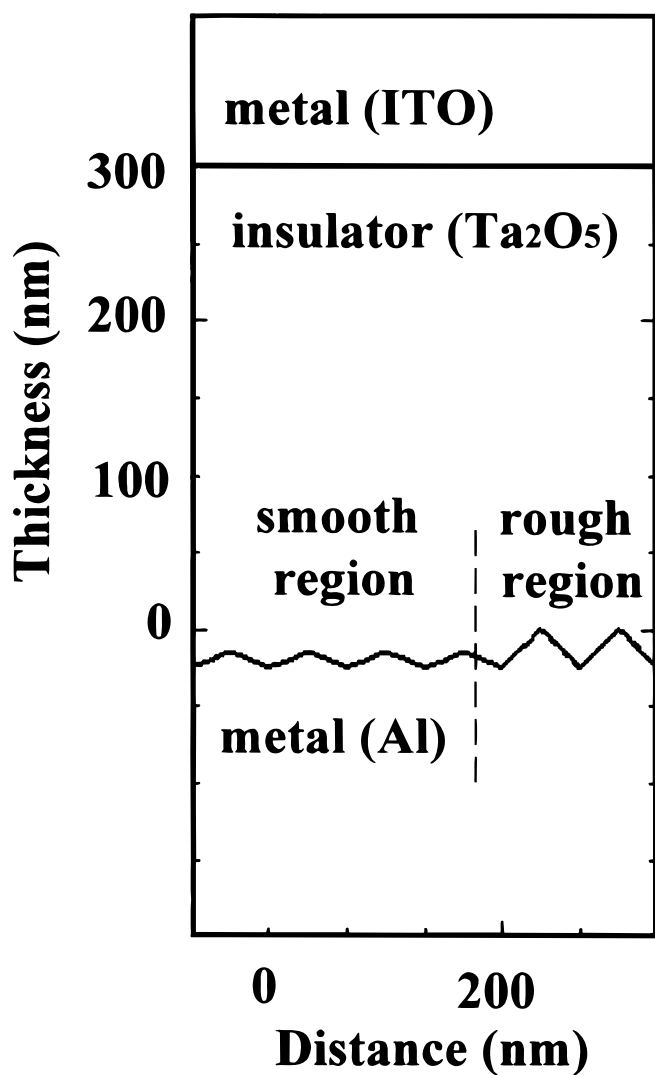


Figure 9. Schematic diagram of the simulated metal-insulator-metal structure.

tion in the thin-film bulk and at the surface. The metal-insulator-metal structure was used for 2D numerical device simulation, as displayed in Fig. 9. To investigate the effect of the surface roughness on the electric field, the surface was divided into two regions, a rough region and a smooth region.

Figure 10a and b displays the calculated electric field distribution in the vicinity of the Al/Ta<sub>2</sub>O<sub>5</sub> interface and in the bulk Ta<sub>2</sub>O<sub>5</sub> thin films. The intensity of the electric field is shown in the neighborhood of the interface. Near the ridges of the metal/insulator interface, the electric field is much stronger than in the bulk, especially in the interface region.

The visualization of the electronic roughness<sup>7</sup> is enhanced when the electric field intensity is plotted as a function of the vertical and horizontal dimensions. Clearly, the electronic roughness is subjectively higher for thin films with rougher surfaces. In addition, it is now evident that the electric field is increased at the Al/Ta<sub>2</sub>O<sub>5</sub> interface due to the surface roughness. The higher field at the interface between the metal and insulator can result in the field emission, impact ionization, or higher SE current due to larger interface barri-

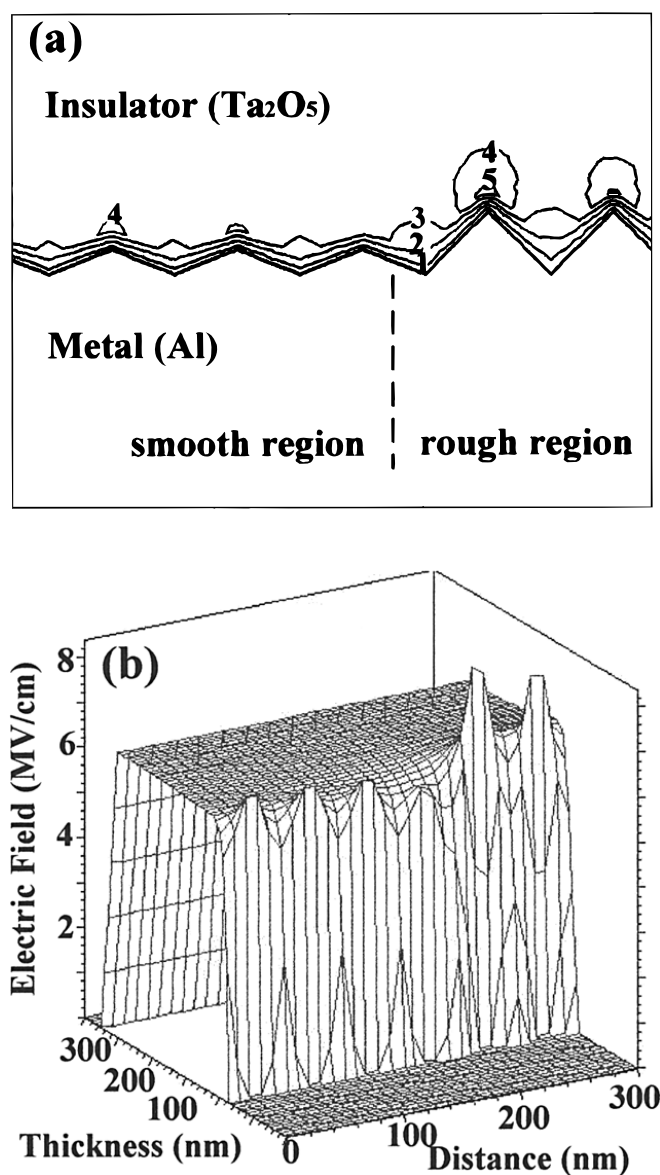


Figure 10. Electric field distribution in the Ta<sub>2</sub>O<sub>5</sub> thin films: (a) electric field contours at the interface between the metal and the insulator and (b) electric field intensity as a function of the vertical (Y) and horizontal (X) dimensions of the metal-insulator-metal structure.

er lowering. It was reported that surface roughness yields on the image potential were as high as even 10-60% compared to that of a flat interface.<sup>9</sup> In these results, the contact resistance of the Ta<sub>2</sub>O<sub>5</sub> thin films with rough interfaces decreases more rapidly with increasing field than that of Ta<sub>2</sub>O<sub>5</sub> thin films with smooth interfaces.<sup>16,17</sup> The leakage current is controlled by a bulk process at lower applied field in the Ta<sub>2</sub>O<sub>5</sub> thin film with a rough interface than with a smooth interface.

In conclusion, the roughness of the Ta<sub>2</sub>O<sub>5</sub> thin film can have an important influence on electrical behavior, especially in the region near the transition from electrode-limited to bulk-limited current.

### Conclusions

The electrical properties of the Ta<sub>2</sub>O<sub>5</sub> thin film obtained by rf-magnetron sputtering were investigated. The leakage current of the Ta<sub>2</sub>O<sub>5</sub> thin films was of the order of 10<sup>-5</sup> to 10<sup>-6</sup> A/cm<sup>2</sup> at an applied field of 1 MV/cm and the charge-storage capacitances ( $\epsilon E_{\text{breakdown}}$ ) are 7.7 (100°C), 7.9 (200°C), and 3.7 (300°C)  $\mu\text{C}/\text{cm}^2$ . With regard to leakage current and charge-storage capacitance, the optimum substrate temperature during deposition was 200°C. The dominant conduction mechanism for amorphous Ta<sub>2</sub>O<sub>5</sub> thin films with 200°C substrate temperature changed from being electrode-limited (SE current) at low field to being bulk-limited (PF current) at high field. To verify the effect of surface roughness on the electric conduction mechanism, a 2D numerical simulator, MEDICI, was used to simulate the electric field distribution in the thin-film bulk. These studies demonstrated that the interface roughness between the

metal and high-dielectric-constant insulating film (Ta<sub>2</sub>O<sub>5</sub>) strongly controlled the current-conduction mechanism and electric field distribution in the insulator. The results suggest that the surface electric fields are modulated by the interface roughness between the metal and dielectric film. The interface roughness of the dielectric and metal layer is one of the physical factors which governs the electrical performance of Ta<sub>2</sub>O<sub>5</sub> thin films.

*Korea University assisted in meeting the publication costs of this article.*

### References

1. K. A. McKinley and N. P. Sandler, *Thin Solid Films*, **290-291**, 440 (1996).
2. T. Shibank and S. H. Rustomji, *Elec. Dev.*, **36**, 1947 (1989).
3. S. Ezhilvalavan and Tseung-Yuen Tseng, *J. Appl. Phys.*, **83**, 4797 (1998).
4. P. L. Young, *J. Appl. Phys.*, **47**, 241 (1976).
5. F.-C. Chiu, J.-J. Wang, J. Y. Lee, and S. C. Wu, *J. Appl. Phys.*, **81**, 6911 (1997).
6. T. Dimitrova and E. Atanassova, *Solid-State Electron.*, **42**, 307 (1998).
7. M. C. Lopes, S. G. dos Santos F., and C. M. Hasenack, *J. Electrochem. Soc.*, **143**, 1021 (1996).
8. H. Tanaka, H. Uchida, N. Hirashita, and T. Ajioka, *IEEE IRPS*, 31 (1992).
9. J. H. Oh, Y. H. Lee, B. K. Ju, D. K. Shin, C. Y. Park, and M. H. Oh, *J. Appl. Phys.*, **82**, 6230 (1997).
10. S. Shibata, *Thin Solid Films*, **277**, 1 (1996).
11. H. Matsumoto, A. Suzuki, and T. Yabumoto, *Jpn. J. Appl. Phys.*, **19**, 71 (1980).
12. E. Kaplan, M. Barlog, and D. Frohman-Bentchkowsky, *J. Electrochem. Soc.*, **123**, 1570 (1976).
13. G. S. Oehrlein, *J. Appl. Phys.*, **59**, 1587 (1986).
14. J. G. Simmons, *Phys. Rev.*, **166**, 912 (1968).
15. G. Palasantzas and J. Krim, *Phys. Rev.*, **73**, 3564 (1994).
16. T. S. Rahman and A. A. Maradudin, *Phys. Rev. B*, **21**, 504 (1980).
17. G. Palasantzas, *J. Appl. Phys.*, **82**, 351 (1997).